
Yan Meng
Hanqi Zhuang

Department of Electrical Engineering
Florida Atlantic University
Boca Raton, FL 33431
zhuang@fau.edu

Self-Calibration of Camera-Equipped Robot Manipulators

Abstract

A new approach to self-calibrate a camera-equipped robot manipulator is proposed in this paper. Self-calibration here means that the camera-robot system is capable of determining its geometric parameters without any external measurements and/or ground truth calibration data. With the proposed approach, one is able to identify all the rotational parameters and, up to a scale factor, all the translational parameters of a robotic system without any ground truth data. It is known from the computer vision literature that the extrinsic and intrinsic parameters of the camera can be obtained up to a scale factor by using the corresponding points of objects in a natural environment from an image sequence without knowing the positions of these object points. It is also well known that if the camera is treated as the tool of the robot, one is able to compute the corresponding robot pose directly from the camera-extrinsic parameters. An important question is how to determine the scale factors, which vary from one robot pose to another. It is discovered in this paper that if the robot pose measurement configurations follow a specially planned optimal trajectory, a unique scale factor can be used for all the poses measured along the trajectory. Thus, one is able to identify all the independent parameters of the robot with the poses measured in this manner with an inherently undetermined scale factor. One question remains: how do we obtain this unknown scale factor? Actually, the problem can be solved in a separate process. By two views of, say, a yardstick with the known length, the scale factor can be computed. If more than one measurement of the scale or measurements of multiple scales are provided from different viewing angles, the scale factor can be estimated with better accuracy in a least squares sense. Extensive simulation and experiment studies on a PUMA 560 robot reveal the convenience and effectiveness of the proposed approach.

KEY WORDS—robot self-calibration, robot autonomous calibration, robot calibration, pose determination, camera self-calibration, motion estimation, structure from motion

1. Introduction

Robot calibration has been an active research area for a number of years. Methods for robot calibration can be categorized into two classes: conventional calibration and self-calibration. In the conventional robot calibration class, reference objects are needed to measure robot poses at various robot measurement configurations (Tsai 1987; Faugeras and Toscani 1986; Weng, Cohen, and Herniou 1992; Zhuang, Wang, and Roth 1993). On the other hand, an ideal self-calibration technique requires no external measurements and/or ground truth calibration data. Self-calibration techniques reported in the literature can be generally classified into the following two subclasses: (1) employ objects such as planes and spheres to constrain the motion of the machine under calibration (Bennett and Hollerbach 1991a, 1991b) (actually, these methods are not self-calibration methods in a strict sense because they use external precision fixtures to provide a sort of ground truth information) or (2) use redundant sensing information provided by sensors installed inside the robot (Zhuang et al. 1992; Zhuang 1997; Zhuang, Liu, and Masory 2000; Khalil and Besnard 1999).

A method for autonomous calibration of serial manipulators was proposed by Bennett and Hollerbach (1991a). By making a fixed contact of a redundant manipulator with a sphere, the resulting parallel kinematic chain is mobile. If the closed loop was moved to a sufficient number of configurations, then joint angle readings could be used to write a sufficient number of loop equations that may be solved to identify all of the relevant kinematic parameters up to a scale factor. The idea was later extended to calibrate a robotic system with a hand-mounted instrumented stereo camera (Bennett and Hollerbach 1991b). The limitation of the algorithm lies in its usage of mechanical constraints (Bennett and Hollerbach 1991a) and the requirement of an instrumented stereo camera (Bennett and Hollerbach 1991b).

A self-calibration technique was proposed in Zhuang et al. (1992) to calibrate a multibeam laser tracking system. Three distance measurements of a single target provided by three laser trackers uniquely determine the location of the target

point in 3-D space. Adding one more distance measurement of the target point provides redundant sensing information, which can be used to find the geometric parameters of the laser system. Zhuang et al., however, did not give explicitly the conditions under which the unknown parameters could be uniquely determined using the measurements from the 4-tracker system.

A framework for the self-calibration of parallel-link mechanisms was proposed in Zhuang (1997). It was pointed out that by using information from redundant sensors, one could formulate forward and inverse residual equations. By minimizing these residuals, kinematic parameters of the mechanism could be identified. The approach was extended in Zhuang, Liu, and Masory (2000), who presented a general approach of creating forward and inverse residual equations and gave experimental results for this algorithm. In this approach, certain passive joints needed to be instrumented. A method for calibrating parallel robots with only measurement information provided by active joint sensors was proposed in Khalil and Besnard (1999). However, the method required the joints to be alternatively locked in the measurement process. Furthermore, only simulation results were provided due to the lack of experimental equipment.

In this study, rather than using measurements from passive joints or imposing mechanical constraints, a wrist-mounted camera, treated as part of a robotic system, was employed as the robot tool. The objective was to develop a new self-calibration algorithm for a robot manipulator without relying on any reference object. We turned our attention to camera self-calibration algorithms developed in the computer vision area. A large amount of work has been reported in the literature about estimating motion parameters of a camera from image sequences (Huang and Netravali 1994). The earlier work mainly focused on the development of linear algorithms and the exploration of the existence and uniqueness conditions of solutions (Faugeras and Maybank 1990; Longuet-Higgins 1981; Tsai and Huang 1984; Hartley 1992). More recently, a number of researchers have proposed algorithms that are noise resistant (Faugeras, Lustman, and Toscani 1987; Loung and Faugeras 1997; Kanatani 1994; Spetsakis and Aloimonos 1989; Weng, Ahuja, and Huang 1993). Although these algorithms are elegant mathematically, most of them are complex and time-consuming in implementation.

Based on the idea in Hartley (1992), an improved nonlinear factor method is proposed in this paper to estimate the camera parameters. However, similar to any other self-calibration method for cameras, one can only estimate the position vector up to a scale factor due to the fact that the system is inherently underdetermined. An approach was given in Meng and Zhuang (2001), in which this scale factor, changing from one camera pose to another, was uniquely determined by a known-length stick located in a place visible by the camera. The limitation of that approach is that the stick has to be used at every robot measurement pose.

It is discovered in this paper that if the robot pose measurement configurations follow a specially planned optimal trajectory, a unique scale factor can be used for all the poses measured along the trajectory. Thus, one is able to identify all the independent parameters of the robot, using poses measured in this manner with only a scale factor undetermined. If desirable, this unknown scale factor can then be determined by using a separate process. By two views of, say, a yardstick with a known length, the scale factor can be computed. If more than one measurement of the scale or measurements of multiple scales are provided from different viewing angles, the scale factor can be estimated with better accuracy in a least squares sense. Extensive simulation and experiment studies on a PUMA 560 robot reveal the convenience and effectiveness of the proposed approach.

The remainder of this paper is organized as follows. In Section 2, preliminaries on self-calibration of a camera and kinematic identification of a robot are given. The materials about estimating the complete pose measurements by using the proposed algorithm are provided in Section 3. Results from simulation and experimental studies are presented in Section 4. Concluding remarks are given at the end of the paper.

2. Preliminaries

2.1. Camera Model

We use perspective projection to model a camera. A projection may be represented by a 3×4 projection matrix \mathbf{P} that incorporates the so-called extrinsic and intrinsic camera parameter (Loung and Faugeras 1997):

$$\mathbf{P} \approx \mathbf{A}[\mathbf{R} \ \mathbf{t}], \quad (1)$$

where \approx means that the equality holds up to a nonzero scale factor; \mathbf{R} and \mathbf{t} , the extrinsic parameters of the camera, are a 3×3 orthogonal matrix representing the camera's orientation and a 3-vector representing its position, respectively; and \mathbf{A} , the intrinsic calibration matrix, is given by

$$\mathbf{A} = \begin{bmatrix} f_x & s & C_x \\ 0 & f_y & C_y \\ 0 & 0 & 1 \end{bmatrix}, \quad (2)$$

where (C_x, C_y) are the coordinates of the principal point; f_x and f_y are the scale factors in image x and y axes, respectively; and s is the parameter describing the skewness of the two image axes. The parameters f_x and f_y are related to the focal length f of the camera.

2.2. Epipolar Transformation

Let a camera take two images by linear projection from two different locations, as shown in Figure 1. Let \mathbf{c} be the optical

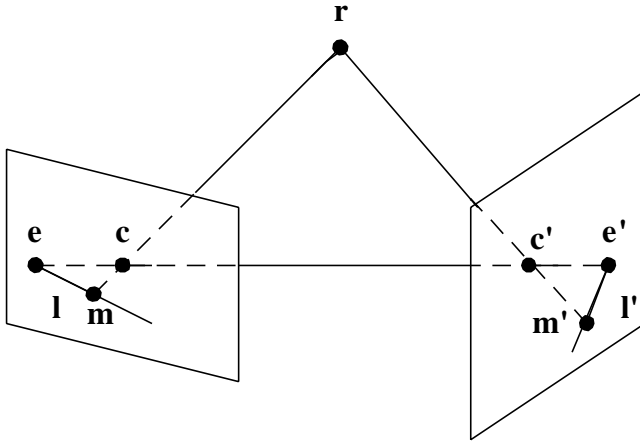


Fig. 1. The epipolar transformation.

center of the camera when the first image is obtained, and let c' be the optical center for the second image. The line $\langle c, c' \rangle$ projects to a point m in the first image and to a point m' in the second image. The lines through e in the first image and the lines through e' in the second image are the epipolar lines. Let r be a point in space, and let m and m' be its two images. The fundamental matrix describes this correspondence: $l' = Qm$. Since point m' corresponding to m belongs to line l' by definition, it follows that (Kanatani 1994)

$$m'^T Qm = 0, \quad (3)$$

where

$$Q = A^{-T} [t]_{\times} R A^{-1}, \quad (4)$$

where $[t]_{\times}$ is an antisymmetric matrix defined as

$$[t]_{\times} = \begin{bmatrix} 0 & -t_z & t_y \\ t_z & 0 & -t_x \\ -t_y & t_x & 0 \end{bmatrix}. \quad (5)$$

2.3. Kinematic Identification

A kinematic error model for robot calibration, which is basically a first-order approximation of the error equation, can be defined as (Zhuang and Roth 1996)

$$\Delta y = J \Delta \rho, \quad (6)$$

where J is the identification Jacobian matrix, Δy is the vector of end-effector pose errors, and $\Delta \rho$ is the vector of independent kinematic link parameter errors. With this error model, link parameter errors can be determined with a nonlinear least squares algorithm. An example using the modified complete and parametrically continuous (MCPC) error model is given in Zhuang and Roth (1996) and Wang (1993).

To obtain superior calibration results with fewer robot measurement configurations, one must carefully plan the robot

motion trajectory at which the robot poses and robot measurement configurations are sampled. An observability measure, which is used to gauge the performance of a set of measurement configurations, can be defined in terms of the condition number of the Jacobian matrix as

$$\text{Cond}(\mathbf{J}) = \sigma_{\max} / \sigma_{\min}, \quad (7)$$

where σ_{\min} and σ_{\max} are the minimum and maximum singular values of \mathbf{J} . Clearly, $\text{Cond}(\mathbf{J}) \geq 1$. Moreover, $\text{Cond}(\mathbf{J}) \cong \infty$ indicates that at least one of the error parameters is unobservable.

3. The Proposed Approach

3.1. The Refined Nonlinear Factor Method

The original factor method to obtain the camera pose data with the uncalibrated camera was proposed by Hartley (1992). This method only uses point correspondences of two images without knowledge of 3-D world coordinates of these points. In order to give the global picture of our self-calibration algorithm, the factor method is outlined first in this section.

Let us make some assumptions first. Assume that the image center and the ratio of the focal length magnifications $\mu = f_y/f_x$ are known a priori. Assume also that lens distortion has been either compensated for or is negligible. Based on these assumptions, the intrinsic matrix given in Faugeras and Toscani (1986) is simplified to the following form:

$$A = \begin{bmatrix} f_x & 0 & 0 \\ 0 & \mu f_x & 0 \\ 0 & 0 & 1 \end{bmatrix}. \quad (8)$$

Let the camera be moved to two different positions, with the first position being situated at the origin of world coordinates. The camera is represented by the transformation from the world coordinate system into the image coordinate system. The two transformations are assumed to be

$$P_1 = A[I \ 0], \quad (9)$$

$$P_2 = A[R \ t],$$

where R is a rotation matrix, t a position vector, and A the intrinsic matrix.

From now on, the camera-intrinsic matrix will be referred to as the above simplified form. The parameter f_x can be estimated by a method analogous to the one described in Hartley (1992). The major difference is that only one camera with the intrinsic matrix given in eq. (8) is used in our case, while two different cameras with $f_{x1} = f_{y1}$ and $f_{x2} = f_{y2}$ were applied in Hartley. After f_x is calibrated, one has the following theorem with regard to the factor method.

THEOREM 1. Suppose the matrix Q can be factored into a product $[t]_{\times} R$, where R is orthogonal and $[t]_{\times}$ is skew symmetric. Let the singular value decomposition of Q be UDV^T ,

where $\mathbf{D} = \text{diag}(n, n, 0)$. Then, up to scale factor k , the factorization is one of the following (Hartley 1992):

$$\begin{aligned} [\mathbf{t}]_{\times} &\approx \mathbf{U}\mathbf{Z}\mathbf{U}^T, \quad \mathbf{R} \approx \mathbf{U}\mathbf{E}\mathbf{V}^T \text{ or } \mathbf{U}\mathbf{E}^T\mathbf{V}^T, \\ \mathbf{Q} &\approx [\mathbf{t}]_{\times}\mathbf{R}, \end{aligned} \quad (10)$$

where \approx means equal to up to a scale factor k , $\mathbf{E} = \begin{bmatrix} 0 & 1 & 0 \\ -1 & 0 & 0 \\ 0 & 0 & 1 \end{bmatrix}$ and $\mathbf{Z} = \begin{bmatrix} 0 & -1 & 0 \\ 1 & 0 & 0 \\ 0 & 0 & 0 \end{bmatrix}$. Given the image corresponding points, the matrix \mathbf{Q} can be calculated by solving eq. (3).

Let us denote $\mathbf{T}_t = [\mathbf{t}]_{\times}$ and $\mathbf{T}_{\hat{t}} = [\hat{\mathbf{t}}]_{\times} = \mathbf{U}\mathbf{Z}\mathbf{U}^T$, where $\hat{\mathbf{t}}$ is the estimated position vector using the factor method. From Theorem 1, the scale factor k can be defined as follows:

$$\mathbf{T}_t = k\mathbf{T}_{\hat{t}}. \quad (11)$$

The original factor method is extremely sensitive to image-related noise. To improve the robustness of the method, one needs to explore a nonlinear least squares procedure. It is natural to minimize the sum of the epipolar distances of the corresponding points in two images from two mapping directions, where the epipolar distance is defined as the distance between the image point and its corresponding epipolar line on the same image.

$$\min_{\mathbf{Q}} \sum_i \left\{ d(\mathbf{m}'_i, \mathbf{Q}\mathbf{m}_i)^2 + d(\mathbf{m}_i, \mathbf{Q}^T\mathbf{m}'_i)^2 \right\}. \quad (12)$$

Considering the fact that $\mathbf{m}'_i{}^T \mathbf{Q}^T \mathbf{m}'_i = \mathbf{m}'_i{}^T \mathbf{Q}^T \mathbf{m}_i$, and replacing \mathbf{Q} with $\mathbf{A}^{-T}[\mathbf{t}]_{\times}\mathbf{R}\mathbf{A}^{-1}$, one has the following cost function:

$$\begin{aligned} \min_{f_x, \mathbf{R}, \mathbf{t}} \sum_i &\left(\frac{1}{(\mathbf{A}^{-T}[\mathbf{t}]_{\times}\mathbf{R}\mathbf{A}^{-1}\mathbf{m}'_i)^2 + (\mathbf{A}^{-T}[\mathbf{t}]_{\times}\mathbf{R}\mathbf{A}^{-1}\mathbf{m}_i)^2} \right. \\ &\left. + \frac{1}{(\mathbf{A}^{-T}[\mathbf{t}]_{\times}\mathbf{R}\mathbf{A}^{-1}\mathbf{m}'_i)^2 + (\mathbf{A}^{-T}[\mathbf{t}]_{\times}\mathbf{R}\mathbf{A}^{-1}\mathbf{m}_i)^2} \right) * \\ &\left(\mathbf{m}'_i{}^T \mathbf{A}^{-T}[\mathbf{t}]_{\times}\mathbf{R}\mathbf{A}^{-1}\mathbf{m}_i \right)^2. \end{aligned} \quad (13)$$

By minimizing the above cost function with the Levenberg-Marquardt nonlinear least squares algorithm in terms of f_x , \mathbf{R} , and \mathbf{t} , the optimal solution may be obtained. Results from the linear factor method can be treated as the initial condition of f_x , \mathbf{R} , and \mathbf{t} in the nonlinear algorithm.

3.2. Determination of the Scale Factor

It has been known that the extrinsic parameters of the camera can only be obtained up to a scale factor based solely on camera position measurements. This scale factor, which differs from one camera pose to another, can be uniquely computed

with a known-length stick (Meng and Zhuang 2001) at each camera pose. In this section, we explore a way to determine the scale factor with a minimum amount of ground truth data with the following fact in mind:

Fact. At least one length scale is required for calibrating any system involving any length measurement. More specifically, the minimum amount of ground truth data for robot self-calibration is the use of a length scale only once.

Based on the above fact, we focus on discovering a way of obtaining a set of robot pose measurements that uses a length scale only once. From the definition of the scale factor obtained from the factor method, one has the following theorem:

THEOREM 2. The ratio of the actual positions of the camera is equal to the ratio of the corresponding scale factors obtained from the factor method:

$$\frac{|k_i|}{|k_{i-1}|} = \frac{\|\mathbf{t}_i\|}{\|\mathbf{t}_{i-1}\|} \quad i = 2, 3, \dots, m, \quad (14)$$

where k_i is the scale factor of the i th movement of the camera, \mathbf{t}_i is the i th actual position vector of the camera, and m is the number of robot pose measurement configurations.

Note: $\|\cdot\|$ means the Frobenius norm throughout this paper unless it is defined otherwise.

Proof. Let us denote $\mathbf{T}_{t_i} = [\mathbf{t}_i]_{\times} = k_i\mathbf{S}_i$ and $\mathbf{S}_i = \mathbf{U}_i\mathbf{Z}\mathbf{U}_i^T$, where $i = 2, 3, \dots, m$, and m is the number of camera displacements. A theorem on the norm of the unitary matrix is provided in Goldberg (1991) as follows: if \mathbf{U} is unitary, then $\|\mathbf{A}\| = \|\mathbf{A}\mathbf{U}\| = \|\mathbf{U}\mathbf{A}\|$.

Since \mathbf{R}_i is a unitary matrix, one has $\|k_i\mathbf{S}_i\mathbf{R}_i\| = \|k_i\mathbf{S}_i\|$. Therefore, one has the following ratios:

$$\begin{aligned} \frac{\|k_i\mathbf{S}_i\mathbf{R}_i\|}{\|k_{i-1}\mathbf{S}_{i-1}\mathbf{R}_{i-1}\|} &= \frac{|k_i| \|\mathbf{S}_i\|}{|k_{i-1}| \|\mathbf{S}_{i-1}\|} \\ &= \frac{|k_i| \|\mathbf{U}_i\mathbf{Z}\mathbf{U}_i^T\|}{|k_{i-1}| \|\mathbf{U}_{i-1}\mathbf{Z}\mathbf{U}_{i-1}^T\|} = \frac{|k_i|}{|k_{i-1}|}. \end{aligned} \quad (15)$$

On the other hand, the above equation can also be expressed as

$$\frac{\|k_i\mathbf{S}_i\mathbf{R}_i\|}{\|k_{i-1}\mathbf{S}_{i-1}\mathbf{R}_{i-1}\|} = \frac{\|k_i\mathbf{S}_i\|}{\|k_{i-1}\mathbf{S}_{i-1}\|} = \frac{\|\mathbf{T}_{t_i}\|}{\|\mathbf{T}_{t_{i-1}}\|}. \quad (16)$$

Thus, the following equation is derived from (15) and (16):

$$\frac{|k_i|}{|k_{i-1}|} = \frac{\|\mathbf{T}_{t_i}\|}{\|\mathbf{T}_{t_{i-1}}\|}. \quad (17)$$

From the definition of the Frobenius norm of the matrix (Watkins 1991),

$$\|\mathbf{A}\|_F = \left(\sum_i \sum_j |a_{ij}|^2 \right)^{1/2}, \quad (18)$$

where a_{ij} ($i = 1, \dots, n, j = 1, \dots, n$) are the entries of the matrix \mathbf{A} . The norm of the vector \mathbf{t} is defined as $\|\mathbf{t}\|_2 = \left(\sum_i^n |t_i|^2\right)^{1/2}$. Therefore, one has

$$\begin{aligned} \|\mathbf{T}_i\| &= \|[\mathbf{t}_i]_\times\| = \left\| \begin{pmatrix} 0 & -t_{iz} & t_{iy} \\ t_{iz} & 0 & -t_{ix} \\ -t_{iy} & t_{ix} & 0 \end{pmatrix} \right\| \\ &= \sqrt{2t_{ix}^2 + 2t_{iy}^2 + 2t_{iz}^2} = \sqrt{2}\|\mathbf{t}_i\|. \end{aligned} \quad (19)$$

From the above equation, one has

$$\frac{\|\mathbf{T}_i\|}{\|\mathbf{T}_{i-1}\|} = \frac{\|\mathbf{t}_i\|}{\|\mathbf{t}_{i-1}\|}. \quad (20)$$

Combining eq. (17) with eq. (20) yields eq. (14). \square

From Theorem 2, it is easy to obtain the following equation:

$$|k_i| = \frac{\|\mathbf{t}_i\|}{\|\mathbf{t}_1\|} |k_1|, \quad i = 2, 3, \dots, m. \quad (21)$$

Based on the fact that at least one length scale is needed for robot pose measurements, the scale factor for the first pose can be uniquely determined by the given length scale, while the other scale factors can be calculated by eq. (21).

Note that the factor method can only estimate the camera pose; therefore, the position vectors we estimate actually refer to the relative position vectors with respect to the first-position vector of the robot pose measurement. The relationship between the position vectors and the robot movement trajectory is shown in Figure 2.

3.3. Optimal Measurement Configuration Selections

From eq. (21), it is clear that to compute the scale factor, one must know the actual position vectors. However, for self-calibration of the robot, the actual position vectors are not provided. Determining the scale factor without using the actual position vectors is the main focus of this section.

It has been assumed that the nominal parameters of the robot are known (these parameters, in general, are provided by the manufacturer). The idea is that if the ratio of the actual position vectors in eq. (21) can be approximated by the nominal position vectors, then one can use the latter to approximate the former since the latter can be computed from the known nominal robot link parameters. The problem is now reduced to design a cost function by which a robot trajectory is chosen to make this approximation valid.

Denote the difference between the nominal and actual position vectors as $\delta\mathbf{t}_i = \mathbf{t}_i - \bar{\mathbf{t}}_i$, where $\bar{\mathbf{t}}_i$ and \mathbf{t}_i are the i th nominal and actual position vectors, respectively. Based on the above discussion, the optimal robot measurement configuration selection problem can be stated as follows.

Determine m robot measurement configurations in the reachable robot joint space such that the following cost function is minimized:

$$\min_{\Theta} \sum_{i=2}^m \left(\frac{\|\bar{\mathbf{t}}_i + \delta\mathbf{t}_i\|}{\|\bar{\mathbf{t}}_{i-1} + \delta\mathbf{t}_{i-1}\|} - \frac{\|\bar{\mathbf{t}}_i\|}{\|\bar{\mathbf{t}}_{i-1}\|} \right), \quad i = 2, 3, \dots, m, \quad (22)$$

where $\Theta^T = [\theta_1, \theta_2, \dots, \theta_m]$ is a set of distinct measurement configurations in the reachable joint space, and $\theta \in \mathbf{R}^n$ is the joint variable vector. Since six equations are obtained from each measurement, a total number of measurements, which provides $6m$ equations, must satisfy the condition $6m > n$, where n is defined as the number of independent kinematic parameters of the robot arm.

To minimize the above cost function, one needs to have $\delta\mathbf{t}_i$, which is again unknown. The following lemma provides a means to solve the problem.

LEMMA 1. Up to a first-order approximation, the following equation holds:

$$\frac{\|\bar{\mathbf{t}}_i\|}{\|\bar{\mathbf{t}}_{i-1}\|} - \frac{\|\bar{\mathbf{t}}_i + \delta\mathbf{t}_i\|}{\|\bar{\mathbf{t}}_{i-1} + \delta\mathbf{t}_{i-1}\|} \cong 0 \quad (23)$$

if

$$\frac{\|\bar{\mathbf{t}}_i\|^2}{\|\bar{\mathbf{t}}_{i-1}\|^2} = \frac{\bar{\mathbf{t}}_i^T \delta\mathbf{t}_i}{\bar{\mathbf{t}}_{i-1}^T \delta\mathbf{t}_{i-1}}. \quad (24)$$

Proof. Denote b as the square of the ratio

$$b = \frac{\|\bar{\mathbf{t}}_i + \delta\mathbf{t}_i\|^2}{\|\bar{\mathbf{t}}_{i-1} + \delta\mathbf{t}_{i-1}\|^2} = \frac{(\bar{\mathbf{t}}_i + \delta\mathbf{t}_i)^T (\bar{\mathbf{t}}_i + \delta\mathbf{t}_i)}{(\bar{\mathbf{t}}_{i-1} + \delta\mathbf{t}_{i-1})^T (\bar{\mathbf{t}}_{i-1} + \delta\mathbf{t}_{i-1})}. \quad (25)$$

Since

$$\begin{aligned} (\bar{\mathbf{t}}_i + \delta\mathbf{t}_i)^T (\bar{\mathbf{t}}_i + \delta\mathbf{t}_i) &= \bar{\mathbf{t}}_i^T \bar{\mathbf{t}}_i + \bar{\mathbf{t}}_i^T \delta\mathbf{t}_i + \delta\mathbf{t}_i^T \bar{\mathbf{t}}_i + \delta\mathbf{t}_i^T \delta\mathbf{t}_i \\ &\cong \bar{\mathbf{t}}_i^T \bar{\mathbf{t}}_i + 2\bar{\mathbf{t}}_i^T \delta\mathbf{t}_i, \end{aligned} \quad (26)$$

$\delta\mathbf{t}_i^T \delta\mathbf{t}_i$ is dropped as it is a second-order term. Substituting eq. (26) into (25), one has

$$b = \frac{\bar{\mathbf{t}}_i^T \bar{\mathbf{t}}_i + 2\bar{\mathbf{t}}_i^T \delta\mathbf{t}_i}{\bar{\mathbf{t}}_{i-1}^T \bar{\mathbf{t}}_{i-1} + 2\bar{\mathbf{t}}_{i-1}^T \delta\mathbf{t}_{i-1}} = \frac{(\bar{\mathbf{t}}_i^T \bar{\mathbf{t}}_i + 2\bar{\mathbf{t}}_i^T \delta\mathbf{t}_i) / (\bar{\mathbf{t}}_{i-1}^T \bar{\mathbf{t}}_{i-1})}{1 + 2 \frac{\bar{\mathbf{t}}_{i-1}^T \delta\mathbf{t}_{i-1}}{\bar{\mathbf{t}}_{i-1}^T \bar{\mathbf{t}}_{i-1}}}. \quad (27)$$

By using Taylor's series, the above equation can be expressed as

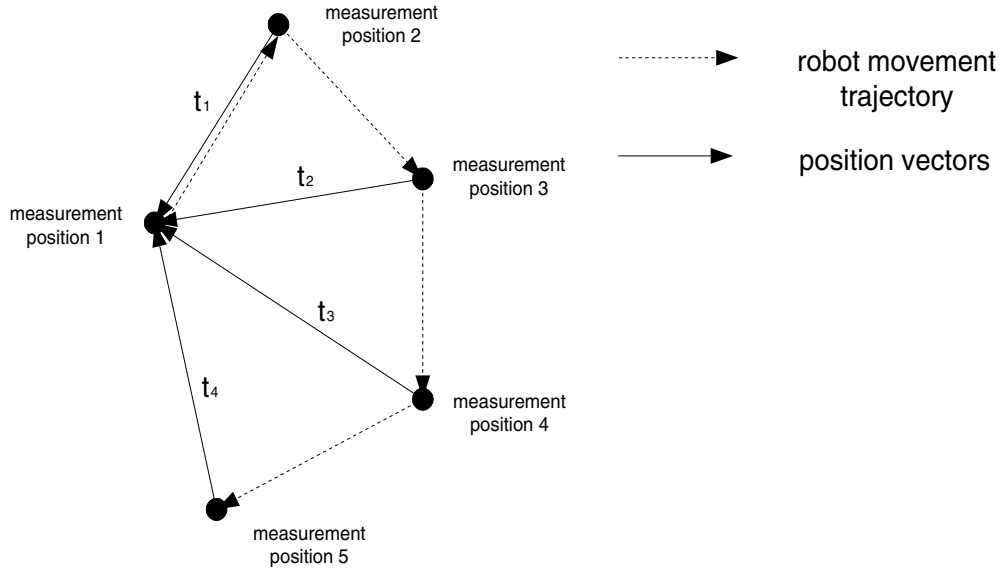


Fig. 2. The robot movement trajectory and position vectors.

$$b = \left(\frac{\bar{\mathbf{t}}_i^T \bar{\mathbf{t}}_i}{\bar{\mathbf{t}}_{i-1}^T \bar{\mathbf{t}}_{i-1}} + 2 \frac{\bar{\mathbf{t}}_i^T \delta \mathbf{t}_i}{\bar{\mathbf{t}}_{i-1}^T \bar{\mathbf{t}}_{i-1}} \right) \left(1 - 2 \frac{\bar{\mathbf{t}}_{i-1}^T \delta \mathbf{t}_{i-1}}{\bar{\mathbf{t}}_{i-1}^T \bar{\mathbf{t}}_{i-1}} + \left(2 \frac{\bar{\mathbf{t}}_{i-1}^T \delta \mathbf{t}_{i-1}}{\bar{\mathbf{t}}_{i-1}^T \bar{\mathbf{t}}_{i-1}} \right)^2 - \dots \right). \quad (28)$$

Removing the second- and higher-order terms from the above equation yields

$$b = \frac{\bar{\mathbf{t}}_i^T \bar{\mathbf{t}}_i}{\bar{\mathbf{t}}_{i-1}^T \bar{\mathbf{t}}_{i-1}} - 2 \frac{\bar{\mathbf{t}}_i^T \bar{\mathbf{t}}_i}{\bar{\mathbf{t}}_{i-1}^T \bar{\mathbf{t}}_{i-1}} \frac{\bar{\mathbf{t}}_{i-1}^T \delta \mathbf{t}_{i-1}}{\bar{\mathbf{t}}_{i-1}^T \bar{\mathbf{t}}_{i-1}} + 2 \frac{\bar{\mathbf{t}}_i^T \delta \mathbf{t}_i}{\bar{\mathbf{t}}_{i-1}^T \bar{\mathbf{t}}_{i-1}}. \quad (29)$$

Substituting (29) into eq. (23), one has

$$\frac{\bar{\mathbf{t}}_i^T \bar{\mathbf{t}}_i}{\bar{\mathbf{t}}_{i-1}^T \bar{\mathbf{t}}_{i-1}} - \frac{\bar{\mathbf{t}}_{i-1}^T \delta \mathbf{t}_{i-1}}{\bar{\mathbf{t}}_{i-1}^T \bar{\mathbf{t}}_{i-1}} - \frac{\bar{\mathbf{t}}_i^T \delta \mathbf{t}_i}{\bar{\mathbf{t}}_{i-1}^T \bar{\mathbf{t}}_{i-1}} = 0. \quad (30)$$

Multiplying $\bar{\mathbf{t}}_{i-1}^T \bar{\mathbf{t}}_{i-1}$ on both sides of the above equation, one has

$$\frac{\|\bar{\mathbf{t}}_i\|^2}{\|\bar{\mathbf{t}}_{i-1}\|^2} = \frac{\bar{\mathbf{t}}_i^T \delta \mathbf{t}_i}{\bar{\mathbf{t}}_{i-1}^T \delta \mathbf{t}_{i-1}}.$$

□

THEOREM 3. Up to a first-order approximation, the cost function given in eq. (22) can be reduced to

$$\min_{\Theta} \sum_{i=2}^m \left(\frac{\bar{\mathbf{t}}_i^T \bar{\mathbf{R}}_i}{\|\bar{\mathbf{t}}_i\|^2} \frac{\partial f(\boldsymbol{\rho}, \boldsymbol{\theta}_i)}{\partial \boldsymbol{\rho}} - \frac{\bar{\mathbf{t}}_{i-1}^T \bar{\mathbf{R}}_{i-1}}{\|\bar{\mathbf{t}}_{i-1}\|^2} \frac{\partial f(\boldsymbol{\rho}, \boldsymbol{\theta}_{i-1})}{\partial \boldsymbol{\rho}} \right). \quad (31)$$

Proof. With Lemma 1, eq. (23) can be rewritten as follows:

$$\frac{\bar{\mathbf{t}}_i^T \delta \mathbf{t}_i}{\|\bar{\mathbf{t}}_i\|^2} = \frac{\bar{\mathbf{t}}_{i-1}^T \delta \mathbf{t}_{i-1}}{\|\bar{\mathbf{t}}_{i-1}\|^2}. \quad (32)$$

Denote the forward kinematic model of the robot as

$$\mathbf{t}_i = f(\boldsymbol{\rho}, \boldsymbol{\theta}_i). \quad (33)$$

where $\boldsymbol{\rho}$ is the robot link parameter vector. Differentiating (33), one has the following equation:

$$d\mathbf{t}_i = \frac{\partial f(\boldsymbol{\rho}, \boldsymbol{\theta}_i)}{\partial \boldsymbol{\rho}} d\boldsymbol{\rho}. \quad (34)$$

It is well known that to a first-order approximation (Zhuang and Roth 1996),

$$\delta \mathbf{t}_i = \bar{\mathbf{R}}_i d\mathbf{t}_i. \quad (35)$$

Combining (34) with (35),

$$\delta \mathbf{t}_i = \bar{\mathbf{R}}_i \frac{\partial f(\boldsymbol{\rho}, \boldsymbol{\theta}_i)}{\partial \boldsymbol{\rho}} d\boldsymbol{\rho}. \quad (36)$$

Substituting eq. (36) into (32) yields

$$\frac{\bar{\mathbf{t}}_i^T \bar{\mathbf{R}}_i}{\|\bar{\mathbf{t}}_i\|^2} \frac{\partial f(\boldsymbol{\rho}, \boldsymbol{\theta}_i)}{\partial \boldsymbol{\rho}} d\boldsymbol{\rho} = \frac{\bar{\mathbf{t}}_{i-1}^T \bar{\mathbf{R}}_{i-1}}{\|\bar{\mathbf{t}}_{i-1}\|^2} \frac{\partial f(\boldsymbol{\rho}, \boldsymbol{\theta}_{i-1})}{\partial \boldsymbol{\rho}} d\boldsymbol{\rho}. \quad (37)$$

It is clear that if

$$\frac{\bar{\mathbf{t}}_i^T \bar{\mathbf{R}}_i}{\|\bar{\mathbf{t}}_i\|^2} \frac{\partial f(\boldsymbol{\rho}, \boldsymbol{\theta}_i)}{\partial \boldsymbol{\rho}} = \frac{\bar{\mathbf{t}}_{i-1}^T \bar{\mathbf{R}}_{i-1}}{\|\bar{\mathbf{t}}_{i-1}\|^2} \frac{\partial f(\boldsymbol{\rho}, \boldsymbol{\theta}_{i-1})}{\partial \boldsymbol{\rho}}, \quad (38)$$

eq. (37) must be satisfied; so must eq. (23). Based on the above derivation, the cost function in (22) can be reduced to eq. (31). \square

Directly applying the cost function in (31) may lead to a singular identification Jacobian. To avoid this from happening, one can add another cost factor into the system. To devise this cost factor, we turn to the concept of observability, which is defined in terms of the identification Jacobian matrix of the robot. It is said that if the Jacobian is nonsingular, the robot link parameter vector is observable; otherwise, it is not observable (Zhuang and Roth 1996). Three major approaches toward quantifying the observability involve an analysis of the singular values: the observability index (Driels and Pathre 1990), the condition number (Borm and Menq 1991), and the minimum singular value (Nahvi, Hollerbach, and Hayward 1994). These three observability measures were applied in Hollerbach and Lokhorst (1995), and it was found that the condition number and the minimum singular value produce about the same results. To a certain extent, the magnitudes of the reciprocal of the condition number were approximately proportional to the RMS errors of the final parameter errors. Therefore, to robustly estimate the link parameter vector, the condition number of the identification Jacobian should be kept small. With this in mind, the overall cost function for the optimal pose measurement configuration selection can be defined as follows:

$$\min_{\Theta} \left\{ \left\| \sum_{i=2}^m \left(\frac{\bar{\mathbf{t}}_i^T \bar{\mathbf{R}}_i}{\|\bar{\mathbf{t}}_i\|^2} \frac{\partial f(\boldsymbol{\rho}, \boldsymbol{\theta}_i)}{\partial \boldsymbol{\rho}} - \frac{\bar{\mathbf{t}}_{i-1}^T \bar{\mathbf{R}}_{i-1}}{\|\bar{\mathbf{t}}_{i-1}\|^2} \frac{\partial f(\boldsymbol{\rho}, \boldsymbol{\theta}_{i-1})}{\partial \boldsymbol{\rho}} \right) \right\| + \lambda \cdot \text{Cond}(\mathbf{J}) \right\}, \quad i = 2, 3, \dots, m, \quad (39)$$

where $\|\cdot\|$ is the Frobenius norm of the matrix, \mathbf{J} is the identification Jacobian matrix, and λ is the weighting factor. The selection of the weighting factor λ depends on the importance of each cost factor. A nonlinear least squares technique can be applied to minimize the above overall cost function. The initial measurement trajectory of this cost function can correspond to a set of feasible configurations in the robot workspace.

4. Experimental Results

4.1. The Implementation Procedure of the Proposed Method

The procedure to implement the proposed method for the self-calibration of robot manipulators is given as follows:

1. Design an optimal pose measurement trajectory with a minimization algorithm described in Section 3.2.
2. Estimate robot pose measurements by using the nonlinear factor method described in Section 2.5, assuming the inherently undetermined scale factor to be 1.
3. Calibrate the robot link parameters with the measured pose measurements.
4. Determine the scale factor in a least squares sense with the measurements from different viewing angles of cameras.
5. Verify the robot calibration results by calculating the 3-D errors in the world coordinate system.

The verification procedure is described as follows. One may compute 3-D world coordinates of each calibration point by using the calibrated robot and camera parameters. This is possible by using more than one view, which is more than one robot configuration of the same calibration point. Two views of an identical point are sufficient to compute its world coordinates by using stereo triangulation. Using more than two views calls for a least squares fitting. Since the only ground truth in our study is the distance of a pair of object points in the world coordinates, the computed distance can be obtained by using the computed world coordinates of this pair of object points. The Euclidian norm of the difference between the computed distance and its given value can be defined as 3-D calibration error.

4.2. Simulation Studies

A robot pose measurement provides six scalar equations for kinematic identification. A total number of required pose measurements must satisfy the condition $6m > n$, where n is the number of independent kinematic parameters of the robot arm. Since there are 30 geometric parameters in the PUMA model, it is clear that at least six measurements are needed for a robust identification of these parameters.

To get more accurate calibration results, 15 robot pose measurement configurations were used to calibrate the robot, and 10 pose measurements were used for verification. The initial measurement samples were generated along a smooth path in the workspace of the robot. A nonlinear least squares method from the Matlab Optimization Toolbox was applied to design an optimal subset of robot measurement configurations from the initial configurations. The value of the damping coefficient λ was varied from 1×10^{-4} to 1×10^{-9} , and it turned out that 1×10^{-7} produced the best result. Therefore, λ was set to be 1×10^{-7} in the simulation. This indicated that the Jacobian matrix in the experimentation was practically well conditioned, and the term associated with the damping coefficient is almost negligible. The procedure for producing an optimal measurement trajectory took about an hour to run using MATLAB on a 150 MHz PC. This calculation time can be reduced drastically with a fast computer. The initial and optimal robot end-effector trajectories in 3-D, as well as the corresponding 2-D coordinates for robot self-calibration, are shown in Figures 3 and 4, respectively. Figure 5 shows the norms of the position vectors.

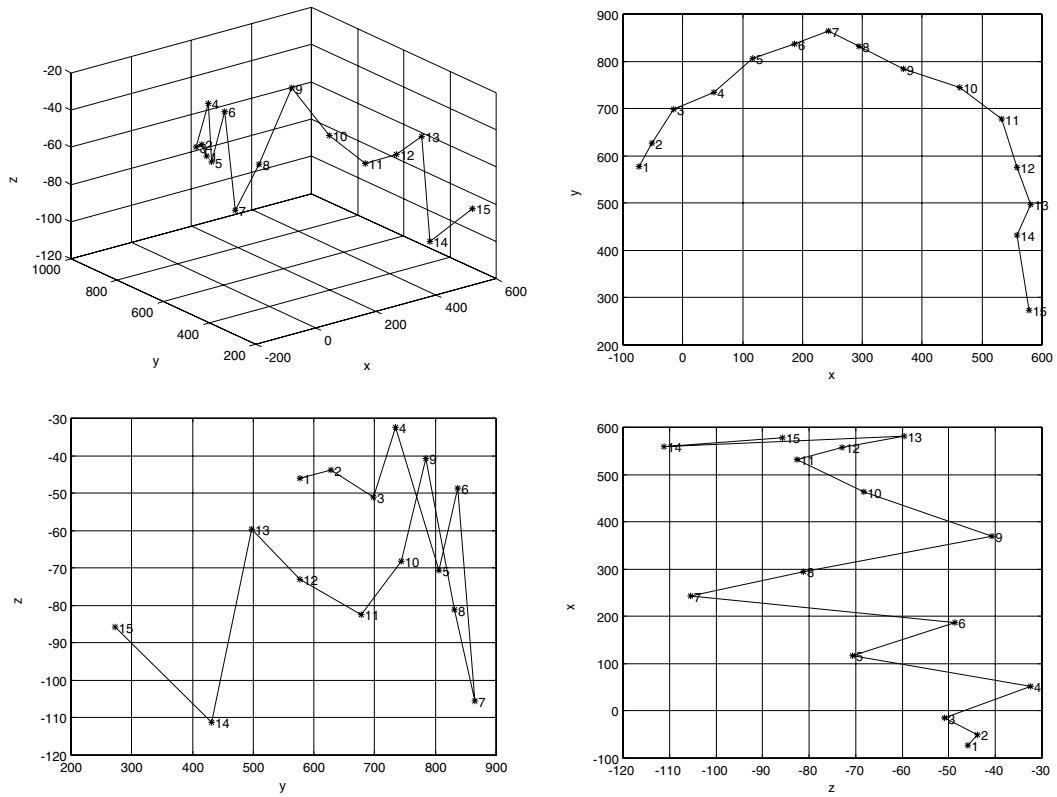


Fig. 3. Initial robot end-effector trajectory for robot calibration.

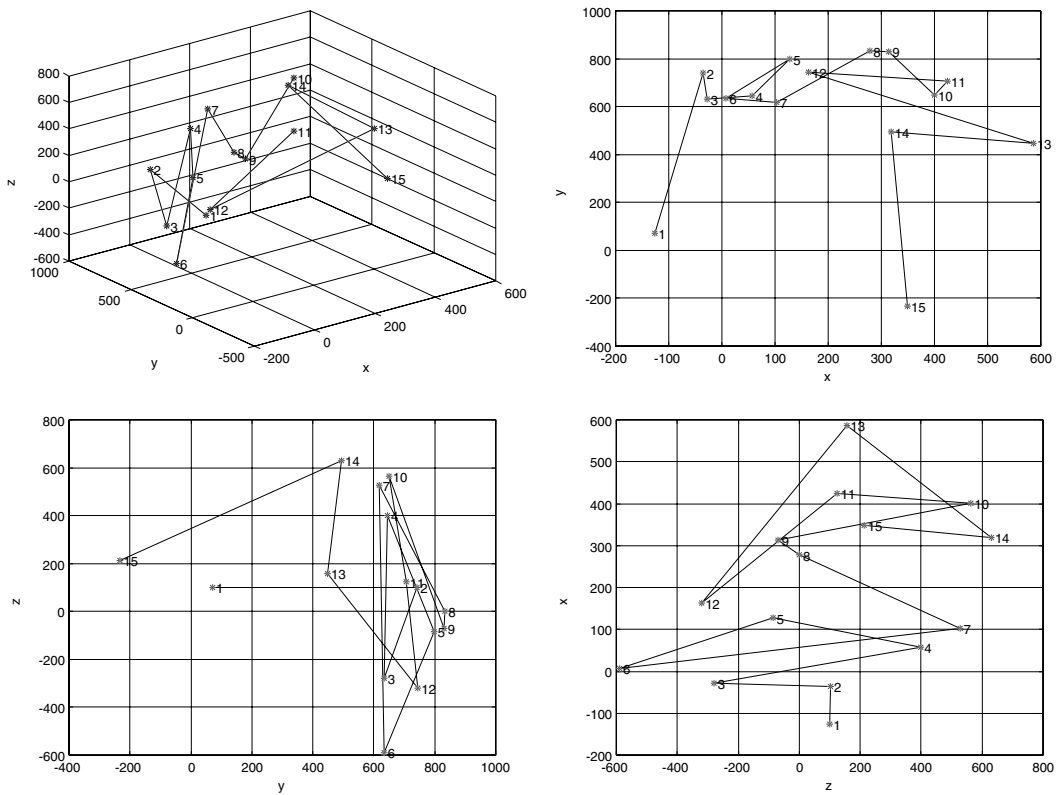


Fig. 4. Optimal robot end-effector trajectory for robot calibration.

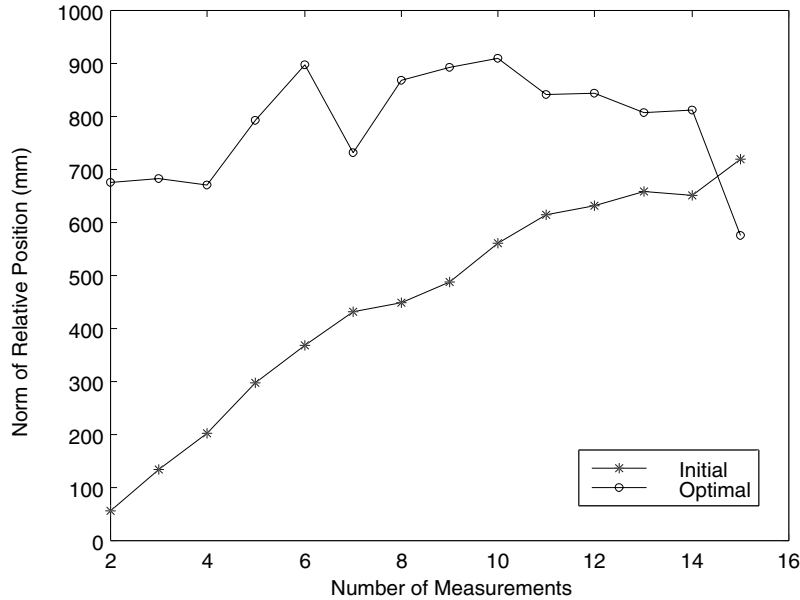


Fig. 5. Norms of the position vectors.

Table 1. Noise Injected to Image Coordinates

Noise Level	Image Noise (pixel)
I	$N(0, 0.2)$
II	$N(0, 0.5)$

Comparing the optimal trajectories with the initial ones in Figures 3, 4, and 5, it can be observed that the distances between the first and the remaining position vectors are larger, and the distances between any two of the remaining position vectors are smaller in the optimal trajectory. This observation does make sense because with the same position vector errors, the larger the position vectors are, the smaller the errors of the ratios given in eq. (23) are. Furthermore, since the position vector errors are defined as the differences between the actual and nominal position vectors, the values of the position vector errors at neighboring pose measurement configurations are intuitively at the same numerical level. Therefore, if the norms of the position vectors are close to each other, the ratio error defined in eq. (23) can be reduced.

Table 1 lists two levels of normally distributed image noise that were used in the simulation, where $N(m, \sigma)$ is the normally distributed function, m is the mean error, and σ is the variance. Table 2 shows pose measurement errors in the presence of two noise levels with initial and optimal trajectories, where 80 points are generated in each simulated image.

Based on the data in Table 2, it is clear that the pose measurement errors increase as the intensity of the image noise increases, and the pose measurement errors obtained from the optimal trajectory decrease significantly compared with those from the initial trajectory, especially the position vector

errors. These simulation results assure us that the proposed algorithm with the designed optimal trajectory is feasible and has superior accuracy performance.

The Levenberg-Marquardt nonlinear least squares algorithm was applied to identify robot link parameters under different simulation conditions with the first 15 pose measurements. The initial condition for the robot link parameters was set as the nominal robot link parameters provided by the manufacturer. The accuracy performance of the algorithm was evaluated by the 3-D errors with the remaining 10 pose measurements. Figure 6 shows the 3-D errors after robot calibration with noise level I and noise level II.

The following observations can be made by analyzing the simulation results:

- As expected, calibration errors increase almost proportionally to the increase of the noise intensity.
- By using more measurements than the required minimum number, estimation errors decrease gradually. This trend slows down significantly after the number of measurements is greater than a certain number.

4.3. Experimental Results

The experiment setup consisted of a PUMA 560 robot, one CCD camera with a 25 mm lens, some non-coplanar calibration dots located within the robot workspace, an RGB (red, green, and blue) color frame grabber DT3154 (made by Data Translation Corp.), and a PC-based image-processing system, as shown in Figure 7a. The calibration object in this case was

Table 2. The Pose Measurement Errors

Trajectory	Position Errors (mm)		Orientation Errors (10^{-4} rad)		f_x Errors (pixel)	
	M	SD	M	SD	M	SD
Initial (I)	3.0427	1.1051	1.4918	2.5354	0.2249	0.2374
Optimal (I)	0.2809	0.2452	1.0701	1.4532	0.1539	0.2128
Initial (II)	6.9837	2.6475	4.0876	7.1762	0.6181	0.7324
Optimal (II)	0.3035	0.2826	2.4016	3.2432	0.3458	0.4791

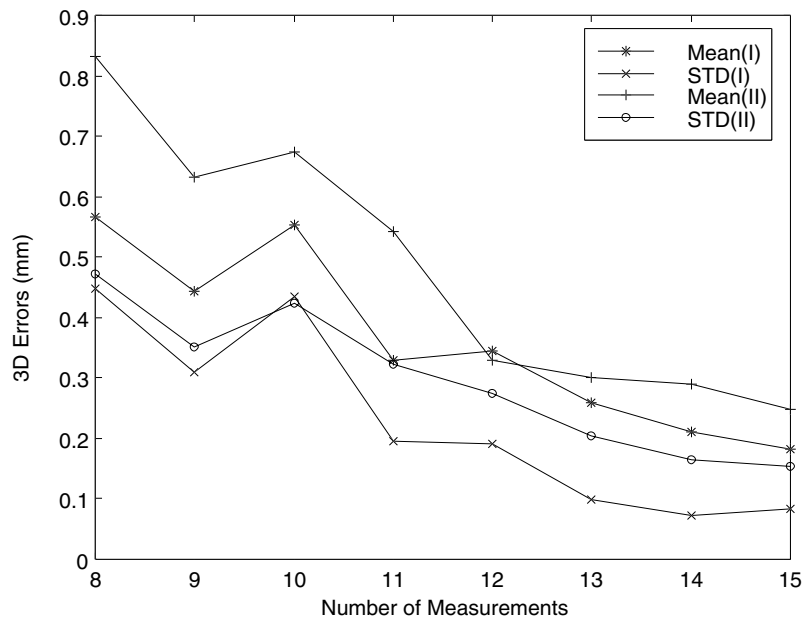
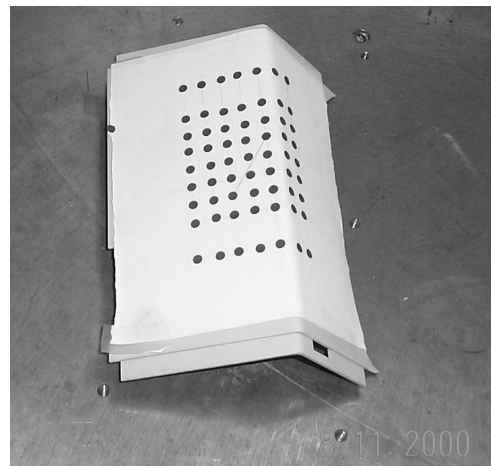


Fig. 6. The 3-D errors after robot calibration.



(a)



(b)

Fig. 7. (a) The measurement system setup. (b) Circular dots used in the experiment.

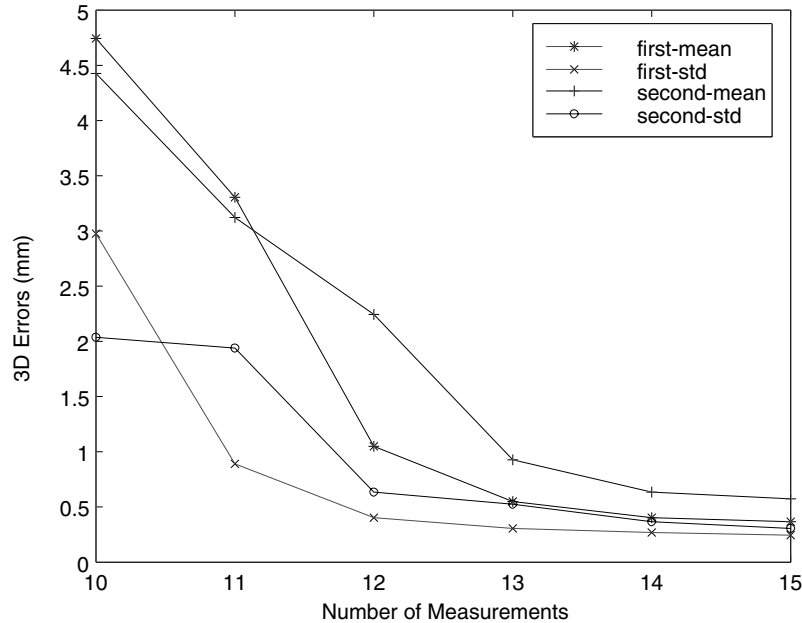


Fig. 8. The 3-D errors after robot calibration.

a dot pattern on letter paper that was pasted on a non-coplanar plastic object, shown in Figure 7b. These dots were made by manually placing circular black stickers on the paper. The positions of these dots were unknown, except for the distance between the two points linked by a line shown in Figure 7b. These two linked points were used to simulate a stick with a known length. Although the dots looked evenly distributed, the sole purpose of arranging these objects in an array was to simplify the correspondence problem in image matching, which was not a focus of our research. The centroid of the corresponding image point of each calibration dot was selected as the estimate of its image coordinates.

To decrease the processing time of obtaining the corresponding points from the images with different camera positions, which is not the focus of our project, the calibration object remains stationary throughout the entire calibration procedure. Therefore, the sampling trajectory needs to be planned due to the limitation of the field of view of the camera.

Since the camera lens distortion is critical for accurate performance of the vision-based calibration system, the camera lens distortion needs to be calibrated separately. For this purpose, a lens distortion calibration algorithm using only the corresponding points of the image has been implemented in our experiment. The experimental result of the lens distortion parameter is 2.996×10^{-8} .

The magnification factors f_x and f_y are fixed for a particular camera vision system; therefore, μ , the ratio of f_x and f_y , needs to be identified only once as long as the same cam-

era vision system is used. A method proposed in Zhuang and Roth (1996) has been applied to estimate μ , which requires the calibration board be moved parallel to itself along a rail, but not necessarily in the direction of the board plane normal. The experimental results turned out that the ratio is equal to 1.00032.

A total of 25 robot pose measurement configurations were recorded. Out of these, 15 pose measurements were used for robot link parameters identification, and the remaining 10 pose measurements were reserved for the purpose of verification. For simplicity, let us denote the method proposed in Meng and Zhuang (2001) as the first algorithm and the method in this paper as the second algorithm. To compare the accuracy performance of these two algorithms, we show the 3-D errors from the verification study with both algorithms in Figure 8.

Due to the limitation that the images of the object points had to be taken by the camera on each robot configuration, the field of view of the camera decreased. Therefore, the pose measurements of the PUMA robot did not exactly follow the trajectory used in the simulation study. Thus, in the actual PUMA calibration, the values of the condition number of the identification Jacobian are higher than those in the simulation case. Since the second algorithm is much more sensitive to the optimal measurement trajectory than the first algorithm, the 3-D errors obtained from the second algorithm are larger than those from the first algorithm (this can be confirmed from Fig. 8). Furthermore, there were more noises involved in the real world during the experiment, such as image detection

errors and lens distortion calibration errors. Consequently, the calibration results obtained from the experiment have a slightly inferior accuracy performance compared with those from the simulation.

5. Concluding Remarks

A new approach to self-calibrate a camera-equipped robot manipulator with a minimum amount of ground truth data was presented in this paper. The approach relies on the camera to acquire robot poses at each robot measurement configuration. However, the measurement provided by the camera can only determine robot poses up to a scale factor. It has been discovered that the inherently unknown scale factors change little from one camera pose to another if the robot follows a carefully designed optimal trajectory. Based on this observation, one is able to identify all the rotational parameters as well as, up to a scale factor, the translational parameters without any ground truth data. This unknown scale factor, if needed, can be computed in a process with additional measurements involving a known yardstick.

To improve the accuracy performance of the proposed self-calibration algorithm, a cost function has been derived for the design of optimal pose measurement trajectories. Other issues related to the optimization algorithm, such as the use of a weighting factor to combine two cost factors and the selection of initial conditions, have also been investigated.

To facilitate practical implementations, extensive simulation and experimental studies have been conducted. Based on these studies, an implementation procedure suitable for a real-world environment has been outlined. These studies have revealed the convenience and effectiveness of the proposed self-calibration approach. The method can be applied to many other situations, such as mobile robot, remote control robot, and autonomous vehicles, due to its minimum usage of the external ground truth data.

A disadvantage of the proposed self-calibration algorithm is that the computation for searching a robot measurement trajectory is intensive, which prevents the method from being used in a real-time application. Nevertheless, this is not a major problem since a calibration task is normally performed off-line.

References

- Bennett, D. J., and Hollerbach, J. M. 1991a. Autonomous robot calibration of single-loop closed kinematic chains formed by manipulators with passive endpoint constraints. *IEEE Transactions on Robotics Automation* 7:597–606.
- Bennett, D. J., and Hollerbach, J. M. 1991b. Autonomous robot calibration for hand-eye coordination. *International Journal of Robotics Research* 10:550–559.
- Borm, J. H., and Menq, C. H. 1991. Determination of optimal measurement configurations for robot calibration based on observability measure. *International Journal of Robotics Research* 10(1):51–63.
- Driels, M. R., and Pathre, U. S. 1990. Significance of observation strategy on the design of robot calibration experiments. *Journal of Robotic Systems* 7:197–223.
- Faugeras, O., Lustman, F., and Toscani, G. 1987. Motion and structure from point and line matches. *Proceedings of the International Conference on Computer Vision*, London, June, pp. 25–34.
- Faugeras, O., and Maybank, S. 1990. Motion from point matches: Multiplicity of solutions. *International Journal of Computer Vision* 4(3):225–246.
- Faugeras, O. D., and Toscani, G. 1986. The calibration problem for stereo. *Proceedings of the IEEE Conference on Computer Vision and Pattern Recognition*, pp. 15–20.
- Goldberg, J. L. 1991. *Matrix Theory with Applications*. New York: McGraw-Hill.
- Hartley, R. 1992. Estimation of relative camera positions for uncalibrated cameras. In *Computer Vision—ECCV'92*, LNCS-Series, Vol. 588, 579–587. New York: Springer-Verlag.
- Hollerbach, J. M., and Lokhorst, D. 1995. Closed-loop kinematic calibration of the RSI 6-DOF hand controller. *IEEE Transactions on Robotics and Automation* 11:352–359.
- Huang, T., and Netravali, A. 1994. Motion and structure from feature correspondences: A review. *Proceedings of IEEE* 82(2):252–268.
- Kanatani, K. 1994. Renormalization for motion analysis: Statistically optimal algorithm. *IEICE Transactions on Information and Systems* E77-D (11):1233–1239.
- Khalil, W., and Besnard, S. 1999. Self calibration of Stewart-Gough parallel robots without extra sensors. *IEEE Transactions on Robotics and Automation* 15(6):1116–1121.
- Longuet-Higgins, H. 1981. A computer algorithm for reconstructing a scene from two projections. *Nature* 293:153–155.
- Loung, Q., and Faugeras, O. 1997. Self-calibration of a moving camera from point correspondences and fundamental matrices. *International Journal of Computer Vision* 22(3):261–289.
- Meng, Y., and Zhuang, H. 2001. Using a stick: Self-calibration of a robot system with factor method. *Proceedings of the IEEE International Conference on Robotics and Automation*, Korea, May.
- Nahvi, A., Hollerbach, J. M., and Hayward, V. 1994. Closed-loop kinematic calibration of a parallel-drive shoulder joint. *Proceedings of the IEEE International Conference on Robotics and Automation*, San Diego, pp. 407–412.
- Spetsakis, M., and Aloimonos, J. 1989. A unified theory of structure from motion. Technical Report CAR-TR-482, Computer Vision Laboratory, University of Maryland.

- Tsai, R. Y. 1987. A versatile camera calibration technique for high-accuracy 3D machine vision metrology using off-the-shelf TV cameras and lenses. *IEEE Journal of Robotics and Automation* RA-3(4):323–344.
- Tsai, R., and Huang, T. 1984. Uniqueness and estimation of three-dimensional motion parameters of rigid objects with curved surface. *IEEE Transactions on Pattern Analysis and Machine Intelligence* 6(1):15–26.
- Wang, K. 1993. Synthesis of vision-based robot calibration using moving cameras. Ph.D. dissertation, Florida Atlantic University, Boca Raton.
- Watkins, D. S. 1991. *Fundamentals of Matrix Computations*. New York: John Wiley.
- Weng, J., Ahuja, N., and Huang, T. 1993. Optimal motion and structure estimation. *IEEE Transactions on Pattern Analysis and Machine Intelligence* 15(9):864–884.
- Weng, J., Cohen, P., and Herniou, M. 1992. Calibration of stereo cameras using a nonlinear distortion model. *IEEE Transactions on Pattern Analysis and Machine Intelligence* 14:965–980.
- Zhuang, H. 1997. Self-calibration of parallel mechanisms with a case study on Steward platform. *IEEE Transactions on Robotics and Automation* 13(3):387–397.
- Zhuang, H., Li, B., Roth, Z. S., and Xie, X. 1992. Self-calibration and mirror center offset elimination of a multi-beam laser tracking system. *International Journal of Robotics and Autonomous Systems* 9:255–269.
- Zhuang, H., Liu, L., and Masory, O. 2000. Autonomous calibration of hexapod machine tools. *Transactions of ASME* 122:140–148.
- Zhuang, H., and Roth, Z. S. 1996. *Camera-Aided Robot Calibration*. Boca Raton: CRC Press.
- Zhuang, H., Wang, L., and Roth, Z. S. 1993. Simultaneous calibration of a robot and a hand-mounted camera. *Proceedings of the IEEE International Conference on Robotics Automation*, Atlanta, GA, May, pp. 149–154.